

See discussions, stats, and author profiles for this publication at: <https://www.researchgate.net/publication/6951294>

Water Dependence of the HO₂ Self Reaction: Kinetics of the HO₂ – H₂O Complex

ARTICLE *in* THE JOURNAL OF PHYSICAL CHEMISTRY A · APRIL 2005

Impact Factor: 2.69 · DOI: 10.1021/jp044592+ · Source: PubMed

CITATIONS

46

READS

65

4 AUTHORS, INCLUDING:



Nozomu Kanno

Meijo University

17 PUBLICATIONS 220 CITATIONS

SEE PROFILE



Mitsuo Koshi

The University of Tokyo

170 PUBLICATIONS 1,779 CITATIONS

SEE PROFILE

Water Dependence of the HO₂ Self Reaction: Kinetics of the HO₂–H₂O Complex

Nozomu Kanno,^{*,†} Kenichi Tonokura,^{†,‡} Atsumu Tezaki,[§] and Mitsuo Koshi[†]

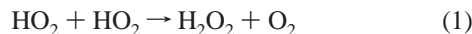
Department of Chemical System Engineering, School of Engineering, The University of Tokyo, Hongo 7-3-1, Bunkyo-ku, Tokyo 113-8656, Japan, Environmental Science Center, The University of Tokyo, Hongo 7-3-1, Bunkyo-ku, Tokyo 113-0033, Japan, and Department of Mechanical Engineering, School of Engineering, The University of Tokyo, Hongo 7-3-1, Bunkyo-ku, Tokyo 113-8656, Japan

Received: November 28, 2004; In Final Form: January 31, 2005

Transient absorption spectra and decay profiles of HO₂ have been measured using cw near-IR two-tone frequency modulation absorption spectroscopy at 297 K and 50 Torr in diluent of N₂ in the presence of water. From the depletion of the HO₂ absorption peak area following the addition of water, the equilibrium constant of the reaction HO₂ + H₂O ↔ HO₂–H₂O was determined to be $K_2 = (5.2 \pm 3.2) \times 10^{-19}$ cm³ molecule⁻¹ at 297 K. Substituting K_2 into the water dependence of the HO₂ decay rate, the rate coefficient of the reaction HO₂ + HO₂–H₂O was estimated to be $(1.5 \pm 0.1) \times 10^{-11}$ cm³ molecule⁻¹ s⁻¹ at 297 K and 50 Torr with N₂ as the diluent. This reaction is much faster than the HO₂ self-reaction without water. It is suggested that the apparent rate of the HO₂ self-reaction is enhanced by the formation of the HO₂–H₂O complex and its subsequent reaction. Results are discussed with respect to the kinetics and atmospheric chemistry of the HO₂–H₂O complex. At 297 K and 50% humidity, the concentration ratio of [HO₂–H₂O]/[HO₂] was estimated from the value of K_2 to be 0.19 ± 0.11 .

1. Introduction

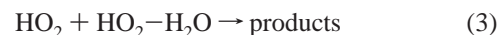
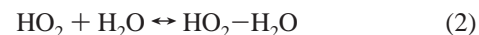
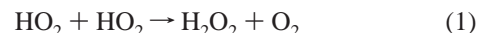
Self-reaction of hydroperoxy radical (HO₂) plays an important role in the atmospheric chemistry of odd hydrogen, HO_x, and is a primary source of hydrogen peroxide in the atmosphere.¹



The kinetics of reaction 1 have been extensively studied both experimentally^{2–11} and theoretically^{12,13} for a wide range of temperatures and pressures. The rate constant of reaction 1 shows a minimum value at around 800 K and a negative temperature dependence below this temperature.¹¹ At around room temperature, the rate constant also shows a pressure dependence with a nonvanishing component at zero pressure.^{4,7,8} These behaviors suggest mechanisms involving an association reaction that results in the formation of an H₂O₄ intermediate, of more or less stability, which fate can then be influenced by collisional energy transfer. Patrick et al.¹² and Mozurkewich and Benson¹³ calculated the temperature and the pressure dependence of the rate constant of reaction 1 based on the above mechanism involving the H₂O₄ intermediate, using the RRKM theory.

Water was found to enhance the rate of reaction 1 more efficiently than it could be explained by the increasing efficiency of the collisional energy transfer of H₂O relative to normal buffer gases such as N₂ and O₂.^{2–4,6–8} Similar enhancements were observed in the case of CH₃OH^{9,10} and NH₃.^{3,5} These species would form hydrogen-bonded HO₂ radical complexes, i.e., HO₂–X (X = H₂O, CH₃OH, and NH₃). These complexes are expected to play an important role in the rate of enhancement

mechanism. Hamilton and Lii³ accounted for H₂O dependence with a multistep mechanism involving a rapid formation of the HO₂–H₂O complex.



Assuming there is an equilibrium between HO₂ and the HO₂–H₂O complex, the rate coefficient of overall radical species (HO₂ and HO₂–H₂O) is expressed as

$$k_{\text{overall}} = \frac{k_1 + k_3 K_2 [\text{H}_2\text{O}] + k_4 (K_2 [\text{H}_2\text{O}])^2}{(1 + K_2 [\text{H}_2\text{O}])^2} \quad (5)$$

where k_1 , k_3 , and k_4 are the rate coefficients of reactions 1, 3, and 4, respectively, and K_2 refers to the equilibrium constant of reaction 2. On the basis of this mechanism, Kircher and Sander⁸ have quantified the rate enhancement with the following expression:

$$k = k_1 \{1 + 1.4 \times 10^{-21} [\text{H}_2\text{O}] \exp(2200/T)\} \quad (6)$$

where [H₂O] refers to the concentration of water in unit of molecule cm⁻³.

Whereas many efforts have been made to estimate k_3 and k_4 ,^{3,4,6} experimental determination of k_3 and k_4 remains difficult due to the large correlation between k_3 and k_4 with K_2 . HO₂ has been conventionally detected by UV absorption in the range 220–230 nm, which shows a structureless feature due to the predissociative $\tilde{B}^2A'' \leftarrow \tilde{X}^2A''$ transition. In this spectral region,

* To whom correspondence should be addressed. E-mail: kanno@chemsys.t.u-tokyo.ac.jp. Fax: +81-3-5841-7488.

[†] Department of Chemical System Engineering.

[‡] Environmental Science Center.

[§] Department of Mechanical Engineering.

the estimation of K_2 is difficult since absorption of the $\text{HO}_2\text{--H}_2\text{O}$ complex would overlap with UV absorption of HO_2 .¹⁴ Using RRKM theory, Mozurkewich and Benson¹³ calculated the values of K_2 and k_3 , assuming that reaction 3 produces the stabilized cyclic H_2O_4 dimer and water, and then the H_2O_4 dimer is excited by collision and dissociates into H_2O_2 and O_2 . They also assumed that the rate constant of reaction 3 is equal to the reaction $\text{HO}_2 + \text{HO}_2\text{--NH}_3$ and fitted the stabilization energy of the $\text{HO}_2\text{--H}_2\text{O}$ complex to experimental results.

In the quantum chemical calculations, Hamilton and Naleway¹⁵ predicted a theoretical hydrogen bonded structure of the $\text{HO}_2\text{--H}_2\text{O}$ complex at the HF/STO-3G level. Aloisio and Francisco¹⁶ calculated the full optimized structure, vibrational spectrum, and binding energy of the $\text{HO}_2\text{--H}_2\text{O}$ complex at several theoretical levels. They estimated the equilibrium constant K_2 to be ca. $10^{-18} \text{ cm}^3 \text{ molecule}^{-1}$ at room temperature, using the binding energy obtained at the CCSD(T)/6-311++G(2df,2p)//B3LYP/6-311++G(2df,2p) level including the correction of the basis set superposition error and the vibrational frequencies at B3LYP/6-311++G(3df,3pd) level of theory. Recently, Lendvay¹⁷ estimated K_2 to be $1.26 \times 10^{-21} \text{ cm}^3 \text{ molecule}^{-1}$ at 290 K at QCISD(T)/6-311++G(2d,2p)//MP2/6-311++G(2d,2p) level including the counterpoise correction. Zhu and Lin^{18–20} calculated the potential energy surfaces of the HO_2 self-reaction and those with $n\text{H}_2\text{O}$ ($n = 1\text{--}3$) at the G2M(CC5)/B3LYP/6-311G(d, p) level of theory. In the presence of water, the reduction of the reaction barrier catalyzed by H_2O was predicted.

In an experimental study, Sander et al.⁷ estimated the reaction yield of H_2O_2 using UV absorption at 227.5 nm. Since HO_2 and H_2O_2 absorb UV light at 227.5 nm, Sander et al. assumed that HO_2 decay followed rigorous second-order behavior and estimated the yield of H_2O_2 from the residual absorption. At 298 K and 500 Torr with O_2 as a diluent, the H_2O_2 yield was estimated to be $[\text{H}_2\text{O}_2]/[\text{HO}_2]_0 = 0.50 \pm 0.12$, which is exactly consistent with the expected stoichiometry of the reaction. Due to the structureless feature of HO_2 and H_2O_2 absorption spectra around 227.5 nm, direct observation of H_2O_2 formation profile is impossible from UV absorption.

To experimentally estimate K_2 , the rovibrational absorption line is preferred for HO_2 detection. Recently, Aloisio et al.²¹ measured HO_2 disappearance using FTIR spectroscopy at the ν_3 band and estimated the K_2 value at 230 and 250 K. They inferred an upper bound of $K_2 = 4 \times 10^{-18} \text{ cm}^3 \text{ molecule}^{-1}$ at room temperature.

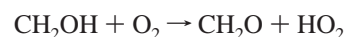
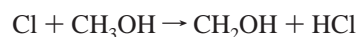
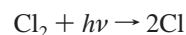
HO_2 shows structured absorption bands in near-IR region.^{22,23} Taatjes and Oh²⁴ detected HO_2 by the $2\nu_1$ band at 6625.8 cm^{-1} using wavelength modulation spectroscopy. Christensen et al.²⁵ also detected HO_2 by the same overtone band at 6638.2 cm^{-1} to study the kinetics of $\text{HO}_2 + \text{NO}_2$. For quantitative detection at the rovibrational absorption line, the influence of pressure broadening must be taken into account. Recently, Kanno et al.²⁶ measured the nitrogen- and water-pressure broadening coefficients of the $\text{HO}_2 \tilde{A}^2A' \leftarrow \tilde{X}^2A'' 000\text{--}000$ band at around 7020.8 cm^{-1} using two-tone frequency modulation (TTFM) absorption spectroscopy. H_2O_2 has a $\nu_1 + \nu_5$ combination band at around 7035 cm^{-1} ,^{27,28} with a rovibrational structure. In this spectral region, HO_2 and H_2O_2 would be expected to be observed as separate absorption lines.

In the present work, we measured the rate enhancement effect of water on HO_2 self-reaction using near-IR TTFM absorption spectroscopy. Using the structured absorption lines of the $\text{HO}_2 \tilde{A}^2A' \leftarrow \tilde{X}^2A'' 000\text{--}000$ band and the $\text{H}_2\text{O}_2 \nu_1 + \nu_5$

combination band, HO_2 decay and H_2O_2 formation were directly observed. From the depletion of the absorption peak area following the addition of water, we determined the equilibrium constant K_2 . Finally, substituting K_2 into the overall decay rate of the HO_2 signal, the rate coefficient of the reaction $\text{HO}_2 + \text{HO}_2\text{--H}_2\text{O}$, i.e., k_3 was estimated.

2. Experimental Section

Near-IR absorption spectra and time profiles of HO_2 and H_2O_2 were measured using laser photolysis/cw TTFM absorption spectroscopy. The apparatus used in the present study has been described in details elsewhere.²⁶ A third harmonics of a Nd:YAG laser at 355 nm (Continuum Surelite II, ca. 110 mJ cm^{-2}) photolyzed Cl_2 , initiating the following reactions that resulted in the formation of HO_2 .



Typical concentrations (molecule cm^{-3}) of the reagents were as follows: for Cl_2 , 3×10^{15} ; for CH_3OH , 4×10^{15} ; for O_2 , 1×10^{16} , and for H_2O , $(0\text{--}4) \times 10^{17}$. Although CH_3OH shows an enhancement effect on the self-reaction rate of HO_2 ,^{9,10} the methanol enhancement effect on the reaction rate is negligible under the present experimental conditions at room temperature.

The near-IR probe beam was generated by a tunable diode laser (New Focus Velocity 6327) that was frequency modulated at two closely spaced radio frequency waves ($599.8 \pm 2.6 \text{ MHz}$) in an MgO:LiNbO_3 crystal housed in an external resonant cavity (New Focus 4423M). The modulated beam passed through a flow reactor and was monitored with an InGaAs photovoltaic detector (New Focus 1811FSM). Differential attenuation of either the carrier or the sidebands unbalances the phase-modulated light and generates a beat note in the detector photocurrent whose amplitude is proportional to the absorption.²⁹ The frequency of the probe beam was measured simultaneously with a wavemeter (Burleigh WA-1500) during spectral and kinetic measurements. The detector photocurrent was heterodyne detected at twice the intermodulation frequency ($2 \times 2.6 \text{ MHz} = 5.2 \text{ MHz}$) and amplified with a low-noise preamplifier (Stanford Research Systems SR560). The resulting signal was averaged with a digital oscilloscope (Tektronix TDS 520A) and transferred to a personal computer via a general purpose-interface bus. Data processing was done by a LabVIEW (National Instruments) based custom-written software.

The reaction cell consisted of a quartz glass tube (46 mm i.d., ca. 1300 mm long) supported at each end by stainless chambers. In the stainless chambers, C-shape gold-coated mirrors with a 750 mm focal length were mounted at a distance of 1474 mm and formed a Herriott cell.^{30,31} The near-IR probe beam entered through the slit of the Herriott mirror and underwent 23 passes and exited through the slit of another mirror. The UV photolysis beam was expanded to 15 mm diameter and was introduced into the reaction cell through the central hole of the Herriott mirror. A overlapping path-length between the pump and probe beams was ca. 640 mm, leading to an effective optical path-length of ca. 15 m ($640 \text{ mm} \times 23$ passes).

Gas flows were regulated by calibrated mass flow controllers (Kofloc 3660). The total pressure was measured near the exit of the flow cell with a capacitance manometer (MKS Baratron 622A). N_2 was used as the buffer gas for all experiments. The

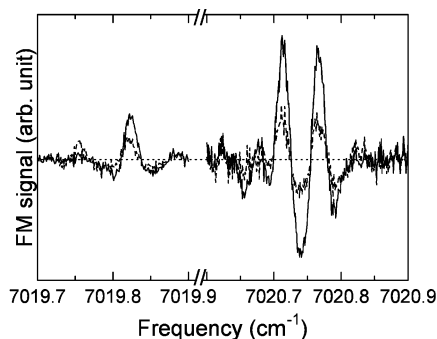


Figure 1. Transient TTFM absorption spectra of Cl₂/CH₃OH/O₂/N₂ mixture. Solid and dashed lines are the spectra obtained at 0–1 and 8–9 ms after photolysis, respectively. The dotted line indicates the zero signal.

gases used in the present experiment were obtained from Nippon Sanso (Cl₂, ca. 10% in N₂; O₂, > 99.99995%; N₂, > 99.99995%). A part of N₂ flow was bubbled through CH₃OH (Wako, research grade) to obtain the desired gas-phase CH₃OH concentration. Reagent concentrations were calculated from the total pressure and the calibrated flow rates. CH₃OH densities in the flow cell were calculated from the pressures in the bubbler and carrier gas flow rates through the bubbler, assuming an equilibrium of the CH₃OH evaporation. A slow N₂ flow was introduced over the optical parts to protect the mirrors and photolysis beam entrance windows, from deposition of reaction products. Kinetic experiments were performed using a laser repetition of 0.5 Hz to ensure removal of the reacted mixture and replenishment of the gas sample between successive laser shots. All experiments were performed at room temperature (297 ± 1 K) and 50 Torr with N₂ as the diluent.

In experimental runs for the investigation of the effects of water addition, a water bubbler was inserted in the gas line. Water concentrations were measured by the near-IR absorption at 7019.754 cm⁻¹. The integrated absorption cross section of this line was referred from the HITRAN database.³² The Doppler-broadening line profile was assumed to estimate the differential absorption cross section at the peak center.

3. Results

The transient absorption spectra of the HO₂ $\tilde{A}^2A' \leftarrow \tilde{X}^2A''$ 000–000 band were observed using TTFM absorption spectroscopy. In this spectral region, H₂O₂, which is a major product of the HO₂ self-reaction, can also be observed at the $\nu_1 + \nu_5$ combination band.^{27,28} For kinetic studies, the absorption line separated from those of other considerable species, such as H₂O₂ and water, is favorable.

Figure 1 shows the part of the transient absorption spectra of HO₂. The solid line indicates the spectrum averaged for 0–1 ms after photolysis. The peak positions of the three strong lines at 7019.823, 7020.713, and 7020.766 cm⁻¹ were in good agreement with the emission spectrum reported by Fink and Ramsay.²³ They assigned these peaks to the 12_{0,12} \leftarrow 11_{1,10} F_2 line, the overlap lines of the 10_{0,10} \leftarrow 9_{1,8} F_1 and 16_{1,16} \leftarrow 16_{0,16} F_2 , and the 16_{1,16} \leftarrow 16_{0,16} F_1 line, respectively. The dashed line shown in Figure 1 indicates the spectrum observed at 8–9 ms after photolysis. At longer delay time, another peak was observed at 7019.757 cm⁻¹. The position of this peak was consistent with the peak assigned to the 9_{1,8} \leftarrow 10_{1,9} line of the H₂O₂ $\nu_1 + \nu_5$ band.²⁸

For the kinetic studies, we chose the 16_{1,16} \leftarrow 16_{0,16} F_1 line of the HO₂ $\tilde{A}^2A' \leftarrow \tilde{X}^2A''$ 000–000 band at 7020.766 cm⁻¹ for the detection of HO₂,²⁶ and the 9_{1,8} \leftarrow 10_{1,9} line of the

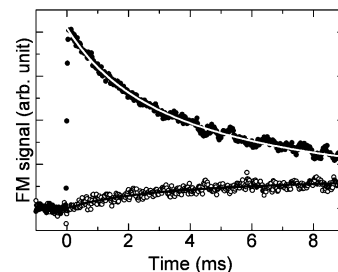


Figure 2. Time profiles of the HO₂ (●) and H₂O₂ (○) signal intensities at 297 K and 50 Torr in diluent of N₂. White and black lines indicate the fitting results.

H₂O₂ $\nu_1 + \nu_5$ band at 7019.757 cm⁻¹ for the detection of H₂O₂. Figure 2 shows the time profiles of the HO₂ and H₂O₂ signal intensities at 297 K and 50 Torr in N₂ as the diluent. The decay profile of HO₂ was well represented by second-order kinetics. Although the initial concentration of HO₂, [HO₂]₀, is required to estimate the rate coefficient of reaction 1, [HO₂]₀ cannot be determined from the signal intensity due to the lack of absorption cross sections of the lines in this absorption band. Therefore, we assumed the rate coefficient of reaction 1 to be $k_1 = 1.86 \times 10^{-12}$ cm³ molecule⁻¹ s⁻¹ at 297 K in 50 Torr with N₂ as the diluent, derived from empirical expression reported by Kircher and Sander,⁸ to determine [HO₂]₀ without water. In the presence of water, [HO₂]₀ was extrapolated using the concentration of Cl₂ and 355 nm photolysis laser power, assuming that both the absorption cross section of Cl₂ and the quantum yield of Cl ($\Phi = 2$) are independent of water concentration. From the decay rate of HO₂ in Figure 2, [HO₂]₀ was estimated to be 7.5×10^{13} molecule cm⁻³. Taking into account the nonlinear least-squares fitting of TTFM absorption spectra (procedures are described latter), the integrated absorption cross section of the 16_{1,16} \leftarrow 16_{0,16} F_1 line of the HO₂ $\tilde{A}^2A' \leftarrow \tilde{X}^2A''$ 000–000 band is estimated to be 9×10^{-22} cm² molecule⁻¹ cm⁻¹. Johnson et al.³³ measured the line strengths of the HO₂ 2 ν_1 overtone band in the 6627 cm⁻¹ region using TTFM spectroscopy under Doppler-limited conditions. They reported the integrated line strength of the strongest line to be 1.6×10^{-21} cm² molecule⁻¹ cm⁻¹. Hunziker and Wendt observed the low-resolution absorption spectrum of HO₂ in the near-IR region.²² In their spectrum, the total peak area of the $\tilde{A}^2A' \leftarrow \tilde{X}^2A''$ 000–000 band roughly equaled that of the 2 ν_1 overtone band. Although the line strength of the 2 ν_1 band reported by Johnson et al.,³³ of which rotational quantum number was unknown, is not strictly comparable to that of the $\tilde{A}^2A' \leftarrow \tilde{X}^2A''$ 000–000 band estimated in the present work, these line strengths are approximately of the same magnitude.

In Figure 2, the absorption signal of H₂O₂ increases with decreasing HO₂ signal. The measurement of HO₂ and H₂O₂ using the separate absorption lines at the near-IR spectral region makes it possible to independently detect these species. The time profile of H₂O₂ signal intensity as a direct product of the HO₂ self-reaction is given by

$$I = I_{\max} \{1 - 1/(1 + 2k[\text{HO}_2]_0 t)\} \quad (7)$$

where I_{\max} and k refer to the signal intensity at infinity time and the second order formation rate of H₂O₂, respectively. The large correlation between I_{\max} and $k[\text{HO}_2]_0$ makes it difficult to determine the precise value of I_{\max} from the nonlinear least-squares fitting of eq 7. To improve accuracy, we fixed the value of $k[\text{HO}_2]_0$ to that obtained from the decay profile of the HO₂ signal. The white and black lines in Figure 2 indicate the fitted results of the time profiles of HO₂ and H₂O₂, respectively.

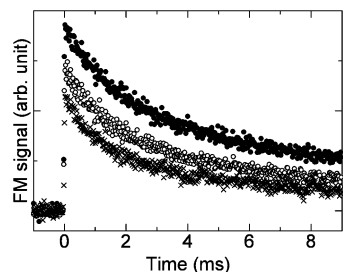


Figure 3. Water dependence of the HO_2 time profiles at 297 K and 50 Torr in diluent of N_2 . $[\text{HO}_2]_0 = 7.73 \times 10^{13}$ molecule cm^{-3} and $[\text{H}_2\text{O}] = 0$ (●), 1.27×10^{17} (○), and 2.97×10^{17} (×) molecule cm^{-3} , respectively.

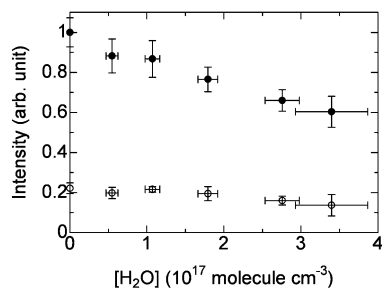


Figure 4. Water dependence of the HO_2 (●) and H_2O_2 (○) signal intensities at 297 K and 50 Torr in diluent of N_2 . Errors are 2σ uncertainties.

In all experiments, the residuals of the fitting curves of eq 7 were uniform within the measured time scale. The agreements between the experimental results and the fitting results on the time profile of H_2O_2 provide the evidence that H_2O_2 is the direct product of the HO_2 self-reaction.

Figure 3 shows typical time profiles of the HO_2 signal following the addition of water. In the presence of water, the HO_2 decay rate was accelerated and the signal intensity was decreased. Figure 4 shows the water dependence of the initial signal intensity of HO_2 and the signal intensity of H_2O_2 at infinity time, I_{max} . The H_2O_2 signal intensity was also reduced with increasing water concentration. The depletion of the signal intensities in Figure 4 would be affected by two factors. One is the formation of the water complexes: $\text{HO}_2\text{--H}_2\text{O}$ and $\text{H}_2\text{O}_2\text{--H}_2\text{O}$, and another is the detection sensitivity in TTFM absorption spectroscopy. In a previous study,²⁶ we found that the pressure broadening coefficients of HO_2 colliding with H_2O were larger than those with N_2 , because of a long-range interaction between HO_2 and H_2O . At constant total pressure diluted with nitrogen, the absorption peaks would be broader with increasing water pressure. The FM signal is proportional to the differential attenuation between the carrier band and the sidebands, and largely affected by the absorption line shape.²⁹

Figure 5 shows typical FM spectra with and without water at 297 K, 50 Torr, with N_2 as the diluent and 0–1 ms after photolysis. On the basis of the theory described by Avetisov and Kauranen,²⁹ the absorption peak shapes were retrieved through nonlinear least-squares fittings assuming the Voigt profile. The details of the fitting procedures were described in our previous paper.²⁶ In the presence of water, the retrieved absorption peak shape was broadened and the corresponding peak area also decreased. From the total area of three peaks appeared in Figure 5, we estimated the corrected signal depletion of HO_2 following the addition of water. Figure 6 shows the water dependence of the HO_2 absorption peak area. HO_2 peak area slightly decreases with increasing water concentration, indicating the formation of the $\text{HO}_2\text{--H}_2\text{O}$ complex.

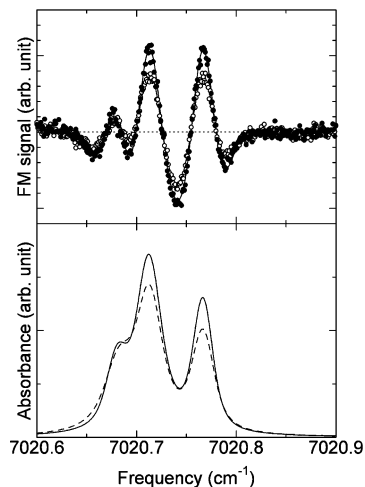


Figure 5. Water dependence of the TTFM spectra (upper panel) and the retrieved absorption spectra (lower panel) of HO_2 at 297 K and 50 Torr with N_2 diluent. Solid circles and solid line exhibit the spectra without water, and open circles and dashed line exhibit those with 2.7×10^{17} molecule cm^{-3} of added water. Dotted line in the upper panel indicates the zero signal.

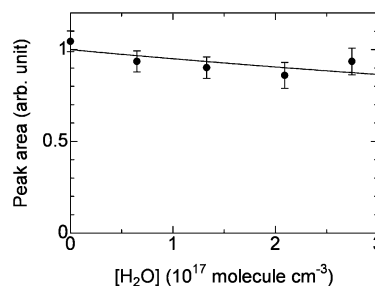


Figure 6. Water dependence of the HO_2 absorption peak area at 297 K and 50 Torr with N_2 as the diluent. Solid line indicates the fitting results. Error bars are one standard errors estimated from the nonlinear least-squares fittings of the TTFM absorption peak shape.

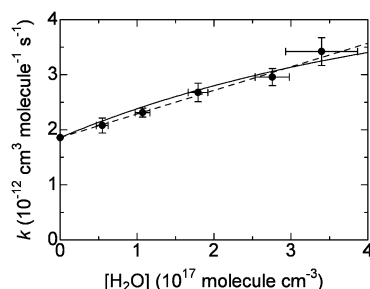


Figure 7. Water enhancement effect of the HO_2 self-reaction. Dashed line indicates eq 6 given by Kircher and Sander.⁸ Solid line indicates nonlinear fitting results from eq 8 (see text). Errors are 2σ uncertainties.

4. Discussion

Prior to discussing the details of the water enhancement mechanism, we first compare our results with previous studies. Figure 7 and Table 1 summarize water dependence of the rate coefficient of the self-reaction of HO_2 at 297 K and 50 Torr with N_2 as the diluent obtained in the present study. Each value represents the average of 3–7 kinetics runs and errors are 2σ uncertainties. In Figure 7, the rate coefficient linearly depended on the water concentration. This behavior well agreed with the dashed line that represents the extrapolated data using the empirical expression reported by Kircher and Sander,⁸ i.e., eq 6.

Although we tried to estimate the kinetics of reaction 2, no divergence from the second-order decay profile was observed in the time scale of sub milliseconds. Thus, the assumption of

TABLE 1: Water Dependence of the HO₂ Self Reaction Rate Coefficient at 297 K and 50 Torr in N₂ as the Diluent

[H ₂ O] ^a	k ^b
0	1.86 ^c
0.55 ± 0.08	2.08 ± 0.14
1.07 ± 0.10	2.31 ± 0.08
1.79 ± 0.12	2.68 ± 0.17
2.76 ± 0.22	2.96 ± 0.15
3.40 ± 0.47	3.42 ± 0.25

^a In units of 10¹⁷ molecule cm⁻³. ^b In units of 10⁻¹² cm³ molecule⁻¹ s⁻¹. ^c Reference 8 (see text).

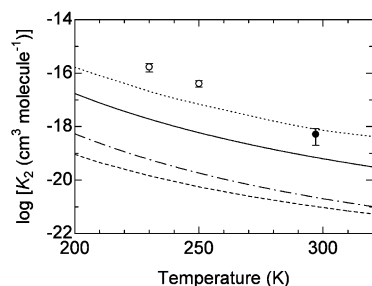


Figure 8. HO₂–H₂O equilibrium constant (K_2) as a function of temperature. The value obtained in the present study is denoted by solid circle. The experimental results from Aloisio et al.²¹ are denoted by open circles. Theoretical estimates reported by Mozurkewich and Benson¹³ (solid line), Aloisio and Francisco¹⁶ (dotted line), Lendvay¹⁷ (dashed line) and Zhu and Lin²⁰ (chained line) are also shown.

the equilibrium of reaction 2 would be valid for the time scale of the present experiments. Based on this assumption, the depletion of the HO₂ peak area following with addition of water is expressed as $A = A_0/(1 + K_2[\text{H}_2\text{O}])$, where A and A_0 refer to the absorption peak area in the presence of water and that without water, respectively. The solid line in Figure 6 indicates the fitting results using this expression. The equilibrium constant of the HO₂–H₂O complex formation was estimated to be $K_2 = (5.2 \pm 3.2) \times 10^{-19}$ cm³ molecule⁻¹ at 297 K. Aloisio et al.²¹ observed the depletion of HO₂ monitored at the ν_3 band in IR region and estimated K_2 at 230 and 250 K. They also inferred the upper bound of K_2 to be less than 4×10^{-18} cm³ molecule⁻¹ at room temperature. The value of K_2 obtained in the present work at 297 K was less than 4×10^{-18} cm³ molecule⁻¹ and consistent with their work. In a kinetic study, Bloss et al.¹⁰ estimated the equilibrium constant of the reaction $\text{HO}_2 + \text{CH}_3\text{OH} \leftrightarrow \text{HO}_2\text{--CH}_3\text{OH}$ to be $(6.15 \pm 0.90) \times 10^{-19}$ cm³ molecule⁻¹ at 298 K. This value was found to be roughly the same as that of K_2 obtained in the present work.

Figure 8 shows the reported values of K_2 as a function of temperature. In theoretical works, the calculated value of K_2 by Aloisio and Francisco¹⁶ was in good agreement with the value obtained in the present experimental work at 297 K. At lower temperatures, their values of K_2 were smaller than the experimentally estimated values reported by Aloisio et al.²¹ The values of K_2 calculated by Mozurkewich and Benson,¹³ Lendvay,¹⁷ and Zhu and Lin²⁰ were smaller than the experimental results.

The water enhancement mechanism of the HO₂ self-reaction kinetics has been explained through the use of the multistep reactions 1–4.^{3,4,6,8} Assuming that equilibrium of reaction 2 occurs, HO₂ decay rate coefficient is expressed by eq 5. The linear dependence of HO₂ decay rate on water concentration shown in Figure 7 indicates that the second-order term in eq 5, $k_4(K_2[\text{H}_2\text{O}])^2$, would be small. Neglecting the contribution of

reaction 4, we get the following equation:

$$k_{\text{overall}} \approx \frac{k_1 + k_3 K_2 [\text{H}_2\text{O}]}{(1 + K_2 [\text{H}_2\text{O}])^2} \quad (8)$$

From the depletion of the absorption peak area following the addition of water, we determined K_2 in the above discussion independently of the kinetic measurements. Fixing K_2 to the value obtained in Figure 6, the rate coefficient of reaction 3 was estimated from the nonlinear least-squares fitting of eq 8. The fitting result is shown in Figure 7 as a solid line.

In the present study, the rate coefficient of the reaction $\text{HO}_2 + \text{HO}_2\text{--H}_2\text{O}$ was estimated to be $k_3 = (1.5 \pm 0.1) \times 10^{-11}$ cm³ molecule⁻¹ s⁻¹ at 297 K, 50 Torr with N₂ as the diluent. Mozurkewich and Benson¹³ reported the rate coefficient to be $k_3 = 1.4 \times 10^{-10}$ cm³ molecule⁻¹ s⁻¹, which is almost equal to the collision frequency. They assumed that the value of k_3 is the same as the rate coefficient of the reaction $\text{HO}_2 + \text{HO}_2\text{--NH}_3$ in the $\text{HO}_2 + \text{HO}_2 + \text{NH}_3$ system, in which the rate enhancement effect is more efficiently observed than that in the $\text{HO}_2 + \text{HO}_2 + \text{H}_2\text{O}$ system. Using the fixed value of k_3 , they fitted the HO₂–H₂O stabilization energy that affects the equilibrium constant K_2 . In the present study, we can separate the value of k_3 from that of K_2 under the fitting procedure, because K_2 value has been independently determined from the water dependence of the rovibronic absorption peak area. The values obtained in the present work suggest that reaction 3 is much faster than reaction 1, i.e., the reaction in the absence of water, but slower than the collision frequencies. The value of k_3 assumed in the work of Mozurkewich and Benson¹³ was roughly 10 times as fast as that estimated in the present work. The large value of k_3 assumed by Mozurkewich and Benson led to a calculated value of K_2 10 times smaller than that obtained in the present work. Bloss et al.¹⁰ studied the CH₃OH dependence of the HO₂ self-reaction over a wide concentration range of CH₃OH. Using a similar analysis, they estimated a rate coefficient of the $\text{HO}_2 + \text{HO}_2\text{--CH}_3\text{OH}$ reaction to be $(3.2 \pm 0.5) \times 10^{-11}$ cm³ molecule⁻¹ s⁻¹ at 298 K and 760 Torr with O₂ as the diluent. Although the estimated rate coefficient is not directly comparable to that of the present work, both values are much larger than the rate coefficient in the absence of water or CH₃OH, i.e., reaction 1. The large value of k_3 suggests that the overall depletion of HO₂ would be accelerated by the formation of the HO₂–H₂O complex and its rapid reaction.

As mentioned by Zhu and Lin,²⁰ the rate enhancement of water on HO₂ self-reaction kinetics is classified following the four mechanisms:

- (i) The formation of the HO₂–H₂O complex and its reaction (the chaperon effect);
- (ii) Reaction with vibrationally excited H₂O₄* complex;
- (iii) Direct termolecular reaction, i.e., $2\text{HO}_2 + \text{H}_2\text{O}$;
- (iv) Reaction with quenched H₂O₄ complex.

The experimental separation of these mechanisms is quite difficult; hence, the value of k_3 obtained in the present work would be a convoluted result. To estimate individual mechanisms, the concentration of the HO₂–H₂O complex must be perturbed by nonthermal processes, such as photolysis.

In Figure 4, the depletion of the H₂O₂ signal intensity with the addition of water was observed. H₂O₂ and water would form the H₂O₂–H₂O complex.³⁴ Furthermore, if the pressure-broadening factors of H₂O₂ colliding with N₂ and water are different in large amounts, the H₂O₂ detection sensitivity in TTFM spectroscopy would be affected by water pressure. To

estimate the H_2O_2 yield dependence on water concentration, we must determine the equilibrium constant of the formation of the $\text{HO}_2\text{--H}_2\text{O}$ complex and the water dependence of the H_2O_2 detection sensitivity. Such observations require further studies.

5. Atmospheric Implications

From the value of K_2 determined in the present work, we can estimate $[\text{HO}_2\text{--H}_2\text{O}]/[\text{HO}_2]$ at various water concentrations. At 297 K and 50% humidity, water concentration in the atmosphere is $[\text{H}_2\text{O}] = 3.6 \times 10^{17}$ molecule cm^{-3} . The concentration ratio of the $\text{HO}_2\text{--H}_2\text{O}$ complex to HO_2 is deduced to be $[\text{HO}_2\text{--H}_2\text{O}]/[\text{HO}_2] = 0.19 \pm 0.11$.

On the assumption that the pressure dependence of reaction 3 is the same as that of reaction 1, the ratio of the HO_2 depletion by reaction 3 to that by reaction 1 is estimated to be $k_3K_2[\text{H}_2\text{O}]/k_1 = 1.5 \pm 1.0$. This result indicates that depletion of more than half the amounts of HO_2 due to the HO_2 self-reaction would proceed through reaction 3. Zhu and Lin^{18–20} predicted that the energy barrier for O_3 formation process would be significantly reduced and would become competitive with the formation of O_2 in the presence of water. The product information of the reactions related to the $\text{HO}_2\text{--H}_2\text{O}$ complex, such as reaction 3, is highly demanded.

The $\text{HO}_2\text{--H}_2\text{O}$ complex might exist in large amounts in the moist troposphere, thus its kinetics would be important. Due to the rapid establishment of the equilibrium of reaction 2, the kinetics of the $\text{HO}_2\text{--H}_2\text{O}$ complex have been commonly recognized as the enhancement effect of the HO_2 kinetics. By determining K_2 by HO_2 detection using the rovibronic absorption line, we can extract the kinetics of the $\text{HO}_2\text{--H}_2\text{O}$ complex from the HO_2 kinetics.

6. Summary

The water enhancement effect on the HO_2 self-reaction has been investigated using near-IR TTFM absorption spectroscopy at around 7020.8 cm^{-1} . Kinetics of both HO_2 and H_2O_2 can be measured at the $\text{HO}_2 \tilde{A}^2A' \leftarrow \tilde{X}^2A'' 000\text{--}000$ band and the $\text{H}_2\text{O}_2 \nu_1 + \nu_5$ band. From the depletion of the HO_2 absorption peak area, the equilibrium constant of the $\text{HO}_2\text{--H}_2\text{O}$ complex formation was determined to be $K_2 = (5.2 \pm 3.2) \times 10^{-19} \text{ cm}^3 \text{ molecule}^{-1}$ at 297 K. Taking into account the K_2 value, the rate coefficient of the reaction $\text{HO}_2 + \text{HO}_2\text{--H}_2\text{O}$ was estimated to be $k_3 = (1.5 \pm 0.1) \times 10^{-11} \text{ cm}^3 \text{ molecule}^{-1} \text{ s}^{-1}$ at 297 K and 50 Torr with N_2 as the diluent. The reaction $\text{HO}_2 + \text{HO}_2\text{--H}_2\text{O}$ would be much faster than the reaction in the absence of water. These results suggested that the overall depletion of HO_2 would be accelerated via the formation of the $\text{HO}_2\text{--H}_2\text{O}$ complex and the subsequent rapid reaction.

Acknowledgment. The authors thank Prof. Thomas Rizzo for providing the PhD Thesis of Bernd Kuhn, and Prof. M. C. Lin for providing reference 20. We also thank Mr. Kotaro Suzuki

and Mr. Masanori Uetake for their assistance in the construction and the improvement of the experimental system. This study was supported by the ministry of Education, Culture, Sports, Science and Technology of Japan Grant-in-Aid for Scientific Research of Priority Areas “A new avenue of radical chain reactions in atmospheric and combustion chemistry”, and Grant for 21st Century COE Program “Center of Excellence for Human-Friendly Materials on Chemistry”.

References and Notes

- (1) Kanaya, Y.; Akimoto, H. *Chem. Rec.* **2002**, 2, 199.
- (2) Hamilton, E. J., Jr. *J. Chem. Phys.* **1975**, 63, 3682.
- (3) Hamilton, E. J., Jr.; Lii, R.-R. *Int. J. Chem. Kinet.* **1977**, 9, 875.
- (4) Cox, R. A.; Burrows, J. P. *J. Phys. Chem.* **1979**, 83, 2560.
- (5) Lii, R.-R.; Gorse, R. A., Jr.; Sauer, M. C., Jr.; Gordon, S. *J. Phys. Chem.* **1980**, 84, 813.
- (6) Lii, R.-R.; Sauer, M. C., Jr.; Gordon, S. *J. Phys. Chem.* **1981**, 85, 2833.
- (7) Sander, S. P.; Peterson, M.; Watson, R. T.; Patrick, R. *J. Phys. Chem.* **1982**, 86, 1236.
- (8) Kircher, C. C.; Sander, S. P. *J. Phys. Chem.* **1984**, 88, 2082.
- (9) Christensen, L. E.; Okumura, M.; Sander, S. P.; Salawitch, R. J.; Toon, G. C.; Sen, B.; Blavier, J.-F.; Jucks, K. W. *Geophys. Res. Lett.* **2002**, 29, art. no. 1299.
- (10) Bloss, W. J.; Rowley, D. M.; Cox, R. A.; Jones, R. L. *Phys. Chem. Chem. Phys.* **2002**, 4, 3639.
- (11) Kappel, Ch.; Luther, K.; Troe, J. *Phys. Chem. Chem. Phys.* **2002**, 4, 4392.
- (12) Patrick, R.; Barker, J. R.; Golden, D. M. *J. Phys. Chem.* **1984**, 88, 128.
- (13) Mozurkewich, M.; Benson, S. W. *Int. J. Chem. Kinet.* **1985**, 17, 787.
- (14) Aloisio, S.; Li, Y.; Francisco, J. S. *J. Chem. Phys.* **1999**, 110, 9017.
- (15) Hamilton, E. J., Jr.; Naleway, C. A. *J. Phys. Chem.* **1976**, 80, 2037.
- (16) Aloisio, S.; Francisco, J. S. *J. Phys. Chem. A* **1998**, 102, 1899.
- (17) Lendvay, G. Z. *Phys. Chem.* **2001**, 215, 377.
- (18) Zhu, R. S.; Lin, M. C. *PhysChemComm* **2001**, 4, 106.
- (19) Zhu, R. S.; Lin, M. C. *Chem. Phys. Lett.* **2002**, 354, 217.
- (20) Zhu, R. S.; Lin, M. C. *PhysChemComm* **2003**, 6, 51.
- (21) Aloisio, S.; Francisco, J. S.; Friedl, R. R. *J. Phys. Chem. A* **2000**, 104, 6597.
- (22) Hunziker, H. E.; Wendt, H. R. *J. Chem. Phys.* **1974**, 60, 4622.
- (23) Fink, E. H.; Ramsay, D. A. *J. Mol. Spectrosc.* **1997**, 185, 304.
- (24) Taatjes, C. A.; Oh, D. B. *Appl. Opt.* **1997**, 36, 5817.
- (25) Christensen, L. E.; Okumura, M.; Sander, S. P.; Friedl, R. R.; Miller, C. E.; Sloan, J. J. *J. Phys. Chem. A* **2004**, 108, 80.
- (26) Kanno, N.; Tonokura, K.; Tezaki, A.; Koshi, M. *J. Mol. Spectrosc.* **2005**, 229, 193.
- (27) Giguère, P. A. *J. Chem. Phys.* **1950**, 18, 88.
- (28) Kuhn, B. Ph.D. Thesis, Ecole Polytechnique Fédérale de Lausanne, France, 1998.
- (29) Avetisov, V. G.; Kauranen, P. *Appl. Opt.* **1996**, 35, 4705.
- (30) Herriott, D.; Schulte, H. *Appl. Opt.* **1965**, 4, 883.
- (31) Trutna, W.; Byer, R. *Appl. Opt.* **1980**, 19, 301.
- (32) Rothman, L. S.; Barbe, A.; Benner, D. C.; Brown, L. R.; Camy-Peyret, C.; Carleer, M. R.; Chance, K.; Clerbaux, C.; Dana, V.; Devi, V. M.; Fayt, A.; Flaud, J.-M.; Gamache, R. R.; Goldman, A.; Jacquemart, D.; Jucks, K. W.; Lafferty, W. J.; Mandin, J.-Y.; Massie, S. T.; Nemtchinov, V.; Newham, D. A.; Perrin, A.; Rinsland, C. P.; Schroeder, J.; Smith, K. M.; Smith, M. A.; Tand, K.; Toth, R. A.; Auwera, J. V.; Varanasi, P.; Yoshino, K. *J. Quant. Spectrosc. Radiat. Transfer* **2003**, 82, 5.
- (33) Johnson, T. J.; Wienhold, F. G.; Burrows, J. P.; Harris, G. W.; Burkhard, H. *J. Phys. Chem.* **1991**, 95, 6499.
- (34) Engdahl, A.; Nelander, B. *Phys. Chem. Chem. Phys.* **2000**, 2, 3967.